Available online at www.sciencedirect.com
ScienceDirect
Catalysis Today 126 (2007) 256–263
CATALYSIS TODAY
www.elsevier.com/locate/cattod

Oxidative dehydrogenation of ethane to ethene on alumina-supported molybdenum-based catalysts modified by vanadium and phosphorus

N. Haddad [a,1], E. Bordes-Richard [b], L. Hilaire [c], A. Barama [a,*]

[a] *Laboratoire de Chimie du Gaz Naturel, Département de Chimie, Faculté des Sciences, USTHB, BP32 El Alia, 16111 Bab Ezzouar, Algiers, Algeria*
[b] *Unité de Catalyse et de Chimie du Solide, UMR CNRS 8181, Université des Sciences et Technologies de Lille, Cité scientifique, 59655 Villeneuve d'Ascq, France*
[c] *ECPM-LMSPC 25, rue Becquerel, 67087 Strasbourg, France*

Available online 26 March 2007

Abstract

Gamma-alumina-supported MoO_x, $MoVO_x$ (Mo/V = 11) and $MoVPO_x$ (Mo/V = 11, V/P = 1) catalysts were prepared and their properties studied by several techniques (EDX-SEM, XRD, XPS, LRS, TPR). Acid–base and catalytic properties were determined by carrying out 2-propanol decomposition and oxidative dehydrogenation of ethane to ethene, respectively. In situ X-ray diffraction and X-ray photoelectron spectroscopy after pre-treatment were carried out in redox conditions (with H_2/N_2, C_2H_6/N_2 as reducing and O_2/N_2 as oxidant). The catalytic performance increases along $MoO_x < MoVO_x < MoVPO_x$ series. Analyses of $MoVPO_x$ show that part of Mo is stabilised as $Al_2(MoO_4)_3$ and that the surface is made up from single or mixed Mo and V oxospecies. Vanadium increases the reducibility of the catalyst as shown by TPD and XPS. Both the acid–base and redox properties are responsible for the catalytic properties of $MoVPO_x$, which are also related to the coordination of Mo active species.

Keywords: Oxidative dehydrogenation of ethane; Vanadia; Molybdena; Structure–activity relationships; In situ experiments

1. Introduction

Olefins are extensively used as intermediates in a large number of industrial syntheses. The oxidative dehydrogenation (ODH) of lower alkanes continues to be an interesting alternative to the endothermic and thermodynamically equilibrated dehydrogenation. The ODH of ethane is a potentially important process to produce ethylene because ethane is relatively more abundant in natural gas and is an inexpensive raw material. For the last two decades, a variety of catalysts containing alkaline, alkaline-earth or rare-earth metal oxides [1–3], or transition metal oxides [4], have been examined in ODH of ethane. Vanadium and molybdenum-based catalysts have been extensively studied in this reaction [5–7]. Mo–V–Nb mixed oxides [8–10], doped with Pd [11–13] or Ca [14], but also supported vanadium oxide [15–18] and VPO and Bi-doped VPO catalysts [19,20] were reported to be active and selective in the partial oxidation of ethane to acetic acid. Impressive yields to ethene of ca. 75% were obtained by using MoVNbTe catalysts [21,22]. In this work, we report on the catalytic performance of γ-Al_2O_3-supported molybdenum-based catalyst modified by vanadium and phosphorus, in ODH of ethane with O_2 as an oxidant. The structural properties of the catalysts have been examined by different techniques before and after catalytic reaction. Their acidity and redox reactivity have also been studied.

2. Experimental

2.1. Materials preparation and characterization

MoO_x catalysts modified by phosphorus and vanadium $MoVPO_x$ (Mo/V = 11 and Mo/P = 11) and $MoVO_x$ (Mo/V = 11), respectively, were supported on γ-Al_2O_3 (samples thereafter called Mo, MoVP and MoV, respectively). In every case, the composition was 15 mol% of active phase with the above stoichiometry (85 mol% of alumina). Samples were prepared by impregnation of γ-Al_2O_3 support (Fluka, 155 m^2/g) with an aqueous solution of $(NH_4)_6Mo_7O_{24}{\cdot}4H_2O$, $(NH_4)_2HPO_4$,

* Corresponding author. Tel.: +213 21 24 79 64; fax: +213 21 24 73 11.
E-mail address: a_barama@yahoo.fr (A. Barama).
[1] Tel.: +213 21 24 79 64; fax: +213 21 24 73 11.

0920-5861/$ – see front matter
doi:10.1016/j.cattod.2007.01.070

NH_4VO_3, in stoichiometric amounts. The impregnated alumina samples were dried in air at 373 K and calcined in a flow (0.55 $cm^3\ s^{-1}$) of dry air at 600 °C for 16 h. Particles to be used in the catalytic reactor were sieved to 180–355 μm.

EDX analysis was carried out in a JEOL JSMS300 scanning electron microscope. Catalyst surfaces were polished with SiC paper.

X-ray powder diffraction (XRD) was performed on Huber D5000 diffractometer using Cu Kα radiation (λ = 0.15418 nm). Patterns were acquired in the range $2\theta = 10–80°$ at room temperature and lines were attributed using the DIFFRACPlus software (Bruker). High temperature diffraction was carried out on a Siemens D5000 diffractometer (Cu Kα radiation), equipped with a HTK 1200 Anton Parr device and a PSD detector. Samples were heated at 0.06 °C s^{-1} in H_2/N_2 = 20/80 and patterns were registered at 300, 350, 400, 450, 500 and 550 °C (30 min at each temperature). After cooling down to room temperature and sweeping by N_2, the sample was reoxidised in O_2/N_2 = 20/80 and then it returned back to room temperature in the same atmosphere.

The laser Raman spectra (LRS) were recorded on Labram infinity laser Raman spectrometer (JY-DILOR) equipped with an optical microscope. The laser intensity (Ar^+, 514.5 nm) was reduced by various filters (<1 mW) and the data were treated by Lasbpec software. The spectral resolution and the accuracy in the Raman shifts are estimated to be 2 cm^{-1}. A tenth particle was examined for each sample to check its homogeneity.

X-ray photoelectron spectroscopy (XPS) was carried out with a LEYBOLD HERAEUS spectrometer using a focused monochromatic Al Kα radiation (13 kV, 20 mA). The pressure was less than 3.10^{-10} Torr in the analyzer system. Samples were preliminary degassed under ultra-high vacuum (10^{-7} Torr) during one night. Post-reaction catalyst samples were sealed in their reactor tubes under He and transferred to a glove box under an inert atmosphere. Samples were then loaded into the analysis chamber without exposure to the atmosphere. In order to observe the effect of reduction and reoxydation on the valence of Mo, samples were treated by a reducing mixture (C_2H_6/N_2 = 20/80) for 30 min at 450 °C in the pre-treatment chamber of the VG-ESCALAB apparatus and then introduced (without exposure to air) inside the vacuum chamber for acquisition of XPS spectrum. Then the reduced samples were submitted to O_2/N_2 = 20/80 flow for 30 min at 450 °C and examined as before.

Temperature-programmed reduction patterns were obtained on 2910 Micromeritics apparatus. Thirty milligrams of catalyst were loaded and were first treated in argon at room temperature for 1 h. The samples were then contacted with an H_2/Ar mixture (H_2/Ar = 1.5 and total flow of 30 cm^3/min) and heated at 6 °C/min up to 1000 °C. The hydrogen consumption was analyzed by on-line gas chromatography.

The decomposition of isopropanol was studied at 120 °C in a fixed bed continuous flow reactor under atmospheric pressure, using nitrogen as a carrier gas. The feed consisted of 2-propanol (pressure 9 mmHg) and the total flow rate of N_2 was 1 l/h. The analysis of products (propene and acetone) was performed by gas chromatography using FID detection.

2.2. Catalytic testing

The catalytic tests were carried out at atmospheric pressure in a conventional flow system with on-line analysis. The fixed bed quartz reactor was loaded with 0.1 g of catalyst. The reaction conditions were 550 °C and the feed was a mixture of C_2H_6 and air (C_2H_6/O_2 = 1) at contact time τ = 0.9 s. Reactants and products were analyzed using on-line Delsi 121 ML TCD gas chromatographs equipped with Carbosieve SII columns for C_2H_6, C_2H_4, CH_4, CO, CO_2, H_2 analysis. The catalytic activity was determined at the steady state which was reached after 2 h of operation.

3. Results and discussion

3.1. Physicochemical analyses

3.1.1. EDX analyses

EDX analyses showed the homogeneity of Mo, V and P dispersion in the alumina-supported samples (Fig. 1). The intensity of Mo signal is very high as compared to Al signal in the case of MoVP, which indicates that the dispersion of both molybdenum and vanadium is higher on MoVP than on MoV and Mo. Similarly, the vanadium signal is more intense on MoVP than on MoV.

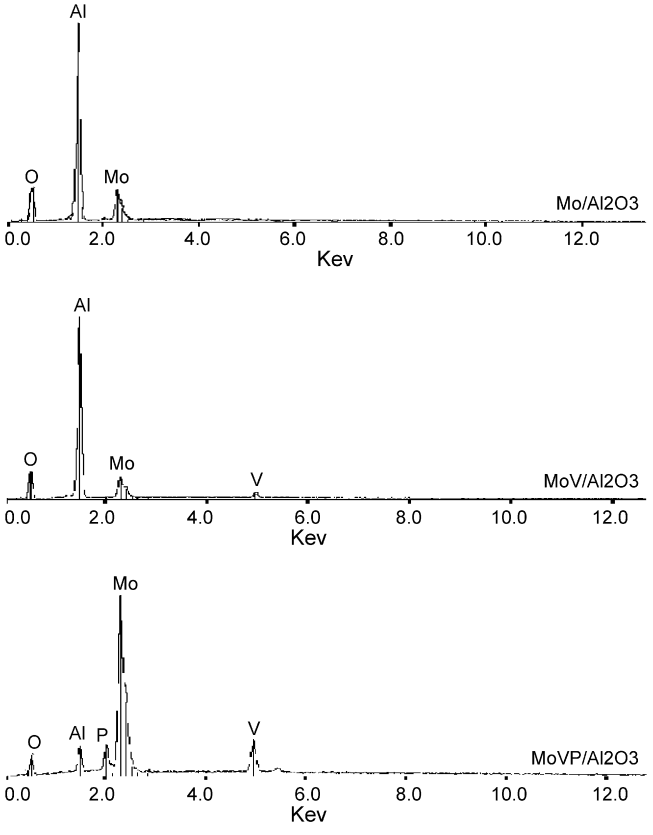

Fig. 1. EDX spectra of alumina-supported Mo, MoV and MoVP calcined catalysts.

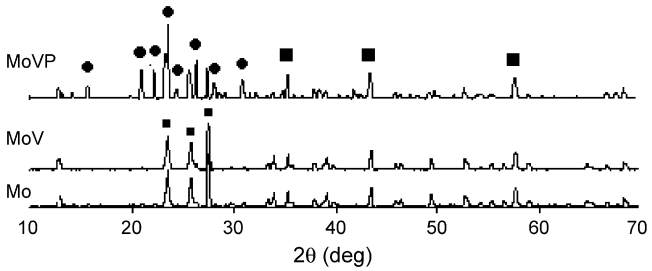

Fig. 2. XRD pattern of alumina-supported Mo, MoV and MoVP calcined at 600 °C. (■) MoO_3;(●) $Al_2(MoO_4)_3$; (■) γ-Al_2O_3.

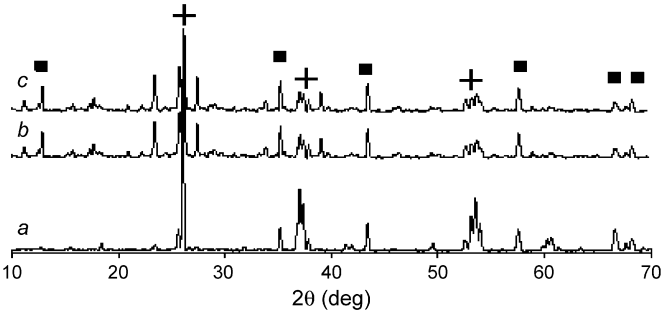

Fig. 3. XRD pattern of alumina-supported Mo, MoV and MoVP after reaction at 550 °C: (●) MoO_2.

3.1.2. X-ray diffraction analysis

The alumina-supported Mo, MoV and MoVP catalysts were analyzed by XRD before and after the catalytic reaction at 550 °C. The pattern of calcined Mo and MoV shows the lines characteristic of the γ-alumina support and of orthorhombic α-MoO_3. The presence of aluminum molybdate $Al_2(MoO_4)_3$ and of γ-alumina is ascertained in calcined MoVP, but no line of MoO_3 nor V_2O_5 is observed (Fig. 2). After the catalytic experiments, Mo catalyst pattern shows lines characteristic of MoO_2 (Fig. 3). More precisely, the solid solution $Mo_{1-x}V_xO_2$ is revealed by weaker lines close to those found in pure MoO_2 in the case of MoV and MoVP. The lines of phosphorus and/or of vanadium oxides or of VPO phases remain however absent in all samples, probably as a result of the good dispersion.

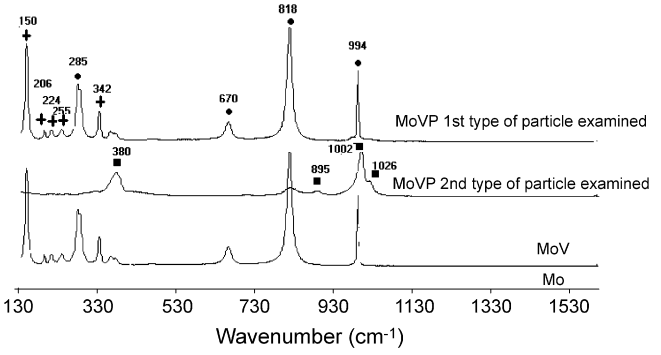

Fig. 4. Raman spectra of alumina-supported Mo, MoV and MoVP calcined catalysts. (△) MoO_3; (●) V_2O_5; (■) $Al_2(MoO_4)_3$.

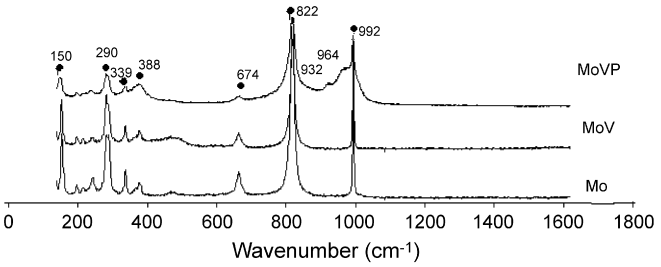

Fig. 5. Raman spectra of alumina-supported Mo, MoV and MoVP used catalysts. (△) MoO_3; (*) additional lines attributed to Mo–V–O phase.

3.1.3. Laser Raman spectroscopy (LRS)

The Raman spectra at room temperature of alumina-supported calcined and used Mo, MoV and MoVP are shown Figs. 4 and 5. The spectrum is the same whichever the observed particles (except the intensity of lines which is different), which means in first approximation that the composition of samples is quite homogeneous. The calcined Mo and MoV samples exhibit Raman lines at 996, 818, 670 and 285 cm^{-1} which are characteristic of α-MoO_3 [23]. In the case of MoVP, two types of spectrum are observed. Besides lines assigned to α-MoO_3, intense lines at 1026, 1002 and weak lines at 895, 828 and 380 cm^{-1} correspond to those of $Al_2(MoO_4)_3$ [24,25]. The presence of aluminum molybdate was already noted in XRD patterns. Lines occurring at 342, 224, 206 and 150 cm^{-1} in MoV and MoVP are related to bulk V_2O_5 [26]. After catalytic reaction, the same type of spectrum than for calcined catalysts is observed. However in the case of MoVP, two additional lines appear at 964 and 932 cm^{-1}. According to Mestl [27] and Roussel et al. [12,13], these lines are assigned to vibrations of Mo–V–O linkages, and more particularly of those in Mo_5O_{14} and hexagonal or orthorhombic molybdenum oxides (e.g. orthorhombic α-$V_xMo_{1-x}O_{3-0.5x}$, $x_{max} = 0.13$) containing minor amounts of vanadium [13,28,29]. Thus, it appears that during the catalytic reaction Mo and V interacts, thereby forming mixed Mo–V–O phases. According to Bañares and Khatib [25], such an interaction is evident in the used catalysts because the mobility of lattice oxygen promotes the interaction between Mo and V during the catalytic redox cycle.

3.1.4. X-ray photoelectron spectroscopy (XPS)

Surfaces of alumina-supported Mo, MoV and MoVP were first analyzed by XPS without any treatment. Hexavalent molybdenum (Mo^{6+}) was detected in all calcined catalysts. Only a slight increase of the binding energy (BE) of the Mo3d3/2 photopeak was observed from 233.0 for Mo to 233.2 for MoV and 233.5 eV for MoVP (Table 1). Reddy et al. [30] showed that

Table 1
XPS results: binding energies and FWHM of Mo-containing catalysts calcined at 600 °C

BE (ev)	Mo^{6+}	V^{5+}	V^{4+}	O1s	FWHM of Mo3d
MoVP	233.5	517.1	516.1	531.1	1.56
MoV	233.2	517.6	516.5	531.3	1.46
Mo	233.0	–	–	531.0	1.44

Table 2
Atomic ratios in calcined alumina-supported Mo, MoV and MoVP determined by XPS compared to theoretical ratios (in brackets)

Catalyst	V/Mo (V/Mo_{th})	V/Al (V/Al_{th})	P/Al (P/Al_{th})	Mo/Al (Mo/Al_{th})
MoVP	0.08 (0.09)	0.35 (0.01)	0.51 (0.02)	4.34 (0.07)
MoV	0.43 (0.09)	0.12 (0.01)	–	0.23 (0.08)
Mo	–	–	–	0.34 (0.09)

a correlation exists between the binding energy of the 3d lines of molybdenum and the coordination of Mo^{6+} species. The formation of $Al_2(MoO_4)_3$ (BE Mo 3d = 233.5 eV) is accounted for by the BE increase when Mo^{6+} coordination changes from octahedral to tetrahedral symmetry. In addition, the Mo 3d photopeak is wider in the MoVP > MoV > Mo series (FWHM: 1.56 > 1.46 > 1.44 eV), in accordance with the presence of Mo^{6+} surface species in various states of coordination [23,31]. Another explanation would be that a strong interaction exists between the active phase and the alumina support.

The decomposition of V2p3/2 photopeak of calcined MoV and MoVP shows the presence of both V^{4+} and V^{5+} species. Nag and Massoth [32] and Haber et al. [33] have hypothesized that the V^{4+} oxidation state is stabilised on Al_2O_3 thanks to the removal of oxygen from the V–O–V linkage in a dimeric surface vanadia species. The values of surface M/Al (M = Mo, V, P) ratio of Mo, MoV and MoVP catalysts (Table 2) are very high as compared to the 'theoretical' values used during preparation, meaning that these elements (Mo, V and P) are localised more on the surface than in the bulk, as expected. In addition, the high value of Mo/Al in the case of MoVP (Mo/Al = 4.34) compared to that in MoV (0.23) and Mo (0.34) confirms that Mo in MoVP is more localised on the external surface than it is in the others. According to Atanasova et al. [34], during the sequential impregnation procedure of MoP/γ-Al2O3 catalysts, acidic P–OH groups are formed on alumina, and they may also enhance the adsorption of Mo species. In such a case, the preferential deposition of molybdenum species on the external surfaces of the catalyst particles has been observed. Strong interaction of $PO4^{3-}$ with alumina may also lead to pore mouth plugging and prevent molybdenum penetration into the support particles. On the other hand, the adsorption of molybdates in the presence of phosphorus oxospecies deposited on an alumina support has been explored by Van Veen et al. [35]. The authors show that the heptamolybdate species interact not only with the OH groups of alumina but also with the P–OH groups (indicated by IR spectra) and lead to the formation of tetrahedral MoO_4^{2-} symmetry according to the surface reaction

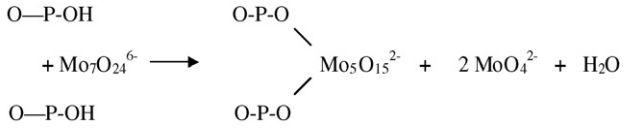

DeCanio et al. [36] and Chadwich et al. [37] reported that the addition of moderate amounts of phosphorus onto Mo/Al catalyst increase the formation of molybdate with a tetrahedral symmetry, this molybdate lead to the formation of $Al_2(MoO_4)_3$ surface on alumina.

3.2. Analysis of the redox behaviour of catalysts

3.2.1. High temperature X-ray diffraction (HT-XRD)

The series of diffraction patterns (Fig. 6) obtained at various temperatures during reduction of MoVP by hydrogen shows that $Al_2(MoO_4)_3$ present at room temperature is stable up to 300 °C. Above this temperature ($T = 400$ °C) the lines characteristic of MoO_2 appear at $2\theta = 26.0°$, 37.0°, 54.0°, while the intensity of lines at 16.2°, 21.4°, 22.7°, 24.6° and 31.0°, characteristic of $Al_2(MoO_4)_3$, decreases. It means that part of $Al_2(MoO_4)_3$ is decomposed to give MoO_2 and Al_2O_3 (Fig. 6). On the other hand, at the same temperature (400 °C) the lines characteristic of $V_xMo_{1-x}O_2$ ($x_{max} = 0.12$) solid solution appear at 37.8° and 54.3°. This result confirms those found by LRS, which showed the lines assigned to vibrations of Mo–V–O linkages for MoVP sample (Fig. 5). The formation of this solid solution was observed by Bouchard et al. [12] during in situ XRD reduction of MoVNb samples at 400 °C. The authors suggested that niobium probably favours the incorporation of vanadium into molybdenum lattice, because this solid solution was not formed in the absence of niobium. In this way and according to this result, the phosphorus could assist the formation of this solid solution in MoVP. By reoxidation at 450 °C in air, lines at 26.8°, 37.0°, 41.5° and 53.8° of α-MoO_3 are observed, besides lines of Al_2O_3. Lines of vanadium or phosphorus oxides or of V–P–O phases remain absent. This

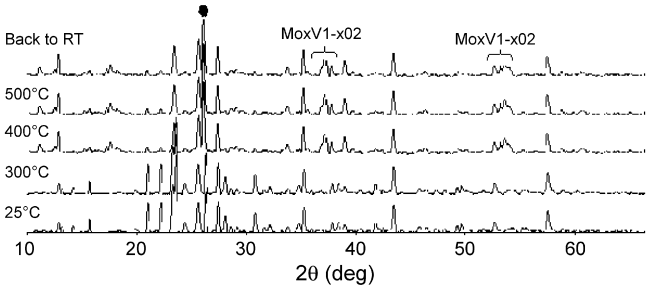

Fig. 6. XRD patterns of in situ reduction of alumina-supported MoVP in H_2/N_2 atmosphere at various temperatures. (● MoO_2 or $V_xMo_{1-x}O_2$).

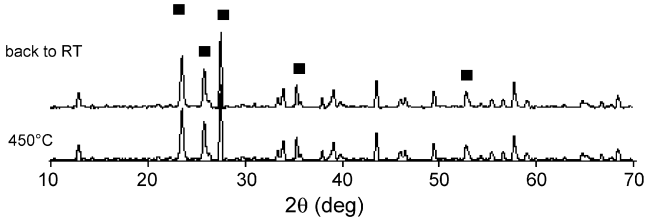

Fig. 7. XRD patterns of the reoxidation of reduced alumina-supported MoVP (■: MoO_3).

Table 3
Atomic ratios and stoichiometry of alumina-supported Mo, MoV and MoVP catalysts obtained by in situ XPS analysis, after calcination at 600 °C (a), after reduction by ethane at 450 °C (b), and after reoxidation by air at 450 °C (c)

Catalyst	V/Mo	V/Al	V/P	Mo/Al	V^{4+}/V_{tot}	V^{4+}/Mo	Surface stoichiometry[α]
MoVP							
a[β]	0.08	0.35	0.68	4.34	0.33	0.02	$Mo_{11}V^{5+}_{0.59}V^{4+}_{0.29}P_{1.30}Al_{2.53}$
b	0.12	0.49	0.73	3.95	0.33	0.03	$Mo_{11}V^{5+}_{0.88}V^{4+}_{0.44}P_{1.80}Al_{2.78}$
c	0.20	0.75	0.91	3.66	0.09	0.02	$Mo_{11}V^{5+}_{2.00}V^{4+}_{0.20}P_{2.4}Al_{3.00}$
Th. ratio[γ]	0.09	0.01	1.00	0.07	–	–	$Mo_{11}V^{5+}_{1}P_1Al_{116.2}$
MoV							
a	0.43	0.12	–	0.23	0.13	0.06	$Mo_{11}V^{5+}_{4.11}V^{4+}_{0.61}Al_{47.8}$
b	0.44	0.10	–	0.21	0.41	0.14	$Mo_{11}V^{5+}_{2.85}V^{4+}_{1.98}Al_{52.4}$
c	0.56	0.12	–	0.21	0.28	0.16	$Mo_{11}V^{5+}_{4.43}V^{4+}_{1.72}Al_{52.4}$
Th. ratio	0.09	0.01	–	0.08	–	–	$Mo_{11}V^{5+}_{1}Al_{137.5}$
Mo							
a	–	–	–	0.34	–	–	$Mo_{11}O_{0.53}Al_{32.3}$
b	–	–	–	0.43	–	–	$Mo_{11}O_{0.51}Al_{25.6}$
c	–	–	–	0.38	–	–	$Mo_{11}O_{0.58}Al_{29}$
Th. ratio	–	–	–	0.09	–	–	$Mo_{11}Al_{122.2}$

[α] O stoichiometry omitted.
[β] a: initial; b: after reduction; c: after reoxidation.
[γ] Theoretical ratios and stoichiometry.

absence is probably related to the strong dispersion of the Mo, V, P elements (Fig. 7).

3.2.2. X-ray photoelectron spectroscopy

The atomic ratios and the stoichiometries obtained by comparing the Mo_{3d}, Al_{2p}, V_{2p}, O_{1s} and P_{2p} photopeaks, are presented for calcined, reduced and reoxidised catalysts in Table 3.

3.2.2.1. Reduction by C_2H_6. By reduction of Mo, MoV and MoVP catalysts at 450 °C with C_2H_6, most molybdenum remains as Mo^{6+}. Vanadium (V) is partly reduced to V^{4+} in MoV but not modified in MoVP. The effect of the reduction on the dispersion of Mo, V and P species is much more significant in the case of MoVP as compared to MoV. Indeed, in the case of MoVP, V/Al and P/Al ratios increase strongly at the expense of Mo/Al. This means that, after reduction, Mo is slightly less present in surface layers (or conversely that V and P species are more numerous on the surface). The variation of these ratios is practically negligible in the case of MoV. In addition, when calculating both V^{4+}/Mo ratio and $\Delta = ({V_R}^{4+} - {V_0}^{4+})/{V_0}^{4+}$, where ${V_0}^{4+}$ and ${V_R}^{4+}$ are the initial and after reduction amounts, respectively, it can be seen that $\Delta = 0.25$ in the case of MoVP versus 1.33 in the case of MoV. Therefore, all these results suggest that the presence of P is responsible for the migration of V towards surface and inhibits its reduction.

3.2.2.2. Reoxidation by air. The treatment of catalysts by O_2/N_2 led both to the partial reoxidation of V^{4+} into V^{5+} as shown by the V^{4+}/V_{tot} ratio, which decreases (from 0.33 to 0.09 in the case of MoVP, and from 0.41 to 0.28 in the case of MoV/Al), and to the migration of more V and P species towards the MoVP surface.

3.3. Temperature-programmed reduction measurements

The study of the reducibility of the alumina-supported Mo, MoV and MoVP catalysts was carried out by TPR (Fig. 8). To compare the reactivity of the samples, the mass was selected in order to have the same amount of molybdenum. Table 4 presents the maximum temperature of the reduction peaks, and the percentage of reduction calculated from the amount of hydrogen consumed. The reduction begins at ca. 450 °C and increases noticeably above 620 °C, except for Mo in which case the rate is smaller. The percentage of reduction increases along Mo < MoV < MoVP (Table 4), thereby demonstrating that both the addition of vanadium, which is more easily reduced than Mo, and phosphorus leads to an increase of the reducibility of the materials. Sajkowski et al. [38] reported XPS measurements showing that the addition of phosphorus to Mo/Al catalysts increase the amount of easily reducible molybdenum species. They presumed that phosphorus weakens the interaction between molybdates and the alumina surface due to the strong interaction between phosphate and alumina. Lopez-Cordero et al. [39] suggested that phosphorus increases the amounts of easily reducible octahedral molybdates, such as poly-oxo-molybdate multilayers and bulk MoO_3 clusters. On

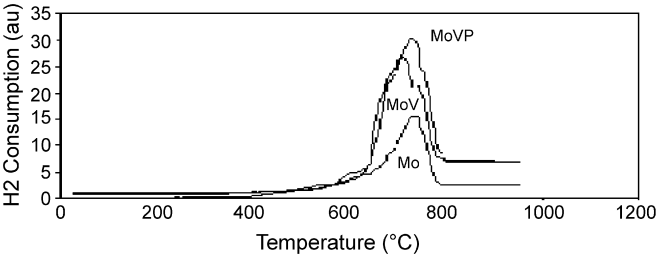

Fig. 8. TPR profiles of alumina-supported Mo, MoV and MoVP catalysts.

Table 4
Characteristic temperatures (range and maximum) of the reduction peaks and percentage of reduction for Mo, MoV and MoVP catalysts

Catalysts	Temperature range (°C)	Temp. maxima (°C)	Percentage of reduction (%)
MoVP	500–800	520, 670, 730, 760	72
MoV	500–790	600, 680, 710, 750	67
Mo	500–790	740	59

Table 5
Catalytic data obtained during oxidation of C_2H_6

Catalysts	C_2H_6 Conv. (%)	O_2 Conv. (%)	Selectivity/mol% (yield/mol%)		
			C_2H_4	CH_4	$CO + CO_2$
MoVP	32.5	62.3	70.0 (22.8)	1.5 (0.5)	28.4 (9.2)
MoV	25.2	55.2	62.3 (15.7)	3.6 (0.9)	34.1 (8.6)
Mo	15.3	43.4	51.6 (7.9)	7.6 (1.2)	40.8 (6.2)

Operating conditions: $T = 550$ °C; $C_2H_6/O_2 = 1$; $\tau = 0.9$ s.

the other hand, Lopez Cordero et al. [40] and Smith et al. [41] associate the reducibility of molybdenum in supported catalysts to the structure of molybdate species. According to these authors, the number of reduction peaks of Mo/γ-Al_2O_3 is related to the different oxospecies of molybdenum which are present on the support surface. In this way, the TPR profiles present one (Mo) or three (MoV, MoVP) maxima between 670 and 790 °C The first peak at ca. 650–680 °C (MoV, MoVP) is attributed to the reduction of octahedrally coordinated molybdenum species weakly bound to Al_2O_3 (polymolybdates), while the peak at ca. 700–730 °C could be assigned to the reduction of microcrystalline MoO_3 to MoO_2. The last peak at ca. 740–760 °C found for the three catalysts is assigned to the partial reduction of molybdenum species (monomolybdate) strongly bound to the support. The reduction of vanadium species could be accounted for by the small peaks at 520 °C (MoVP) and 600 °C (MoV) [42].

3.4. Acid–base and catalytic properties

The catalytic decomposition of 2-propanol was used to determine the acid–base properties of the calcined samples. Propylene, acetone and di-isopropylether were detected. The formation of isopropylether remained negligible on all studied solids. The rates of formation of propylene and of acetone are presented in Fig. 9. For all samples, 2-propanol is predominantly dehydrated to propylene and to a less extent, dehydrogenated to acetone. Both rates of dehydration and dehydrogenation depend on the Mo loading and composition of the samples. The rate of propylene formation, which is an indication of the surface acidic site density, increases with Mo loading along MoVP < MoV < Mo. On the other hand, the acetone formation rate, related to the contribution of redox (basic) site, increases along Mo < MoV < MoVP. The rate is the highest on MoVP catalyst, in accordance with the highest reducibility shown by TPR.

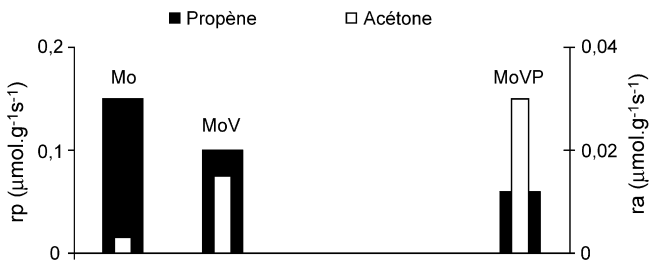

Fig. 9. Rates of formation of propene r_p and of acetone r_a calculated from data of decomposition of isopropanol on alumina-supported Mo, MoV and MoVP catalysts.

The oxidative dehydrogenation (ODH) of ethane on Mo, MoV and MoVP was deliberately performed in such conditions of temperature, contact time and C_2H_6/O_2 ratio that oxygen was not fully converted. The contribution of gas-phase initiated reactions was tested by conducting experiments using an empty-volume reactor. Ethane conversion was null, confirming that gas-phase reactions are negligible under our experimental conditions. The alumina-supported molybdenum-based catalysts are active in the ODH of ethane to ethylene at 550 °C and $C_2H_6/O_2 = 1$ (Table 5). The ethane and oxygen conversions increase along the Mo < MoV < MoVP series. The selectivity to ethylene increases while the selectivity to carbon oxides decreases. The addition of vanadium to Mo (Mo/V = 11) clearly improves both ethane conversion and ethene selectivity, the yield of ethene increasing from 7.9 to 15.7 mol%. This improvement is even more significant in the presence of phosphorus added to MoV (V/P = 1) since the yield increases up to 22.8%. This value places γ-Al_2O_3-supported MoVP among the best catalysts for ODH of ethane.

The difference of catalytic properties of Mo, MoV and MoVP may be accounted for by their redox properties, acid–base character, dispersion of molybdenum, and molybdenum environment. There is a general agreement about the role of redox and surface acid–base properties of catalysts in partial oxidation of light alkanes. Many authors agree that the oxidation reaction proceeds via a Mars and Van Krevelen redox mechanism [43,44], and those early transition metal cations as V, Mo, etc., are necessary because their oxidation state varies in the course of the reaction while O^{2-} oxide ion is inserted in the

reaction product(s). Moreover, it is also accepted that the adsorption and activation of hydrocarbon molecule are related to acid–base interactions, and that the adsorption and desorption rates of products are related to acid–base properties [45]. In agreement with the reactivity of 2-propanol and TPR results, both MoV and MoVP have a higher redox character than Mo catalyst.

The enhancement of the catalytic activity of MoVP as compared to MoV and Mo catalysts could be due to a different dispersion of the Mo active species. Indeed, both XPS and EDX analysis show that Mo is more localised on the external MoVP surface than it is on MoV and Mo surfaces. Smith et al. [41] hypothesized that when direct Mo–O–Al surface linkages are formed (due, for example, to the presence of aluminum molybdate), the Mo dispersion is improved. The presence of $Al_2(MoO_4)_3$ seen by XRD in MoVP, in which case the best Mo dispersion was found, is in accordance with this assumption.

The different activity of the Mo, MoV and MoVP catalysts could be due to a different surface microstructure because of various states of coordination of molybdenum [2]. Apart from the different Mo species (octahedral versus tetrahedral, etc.), both XRD and LRS analyses showed that $Al_2(MoO_4)_3$, which has a beneficial effect on the activation of hydrocarbons [3], is present only in MoVP. Moreover in the latter case, XPS shows that most Al ions (in alumina and/or in aluminum molybdate) are in the bulk (high Mo/Al, Table 2), as compared to MoV and Mo (low Mo/Al).

According to Bañares and Khatib [25], the lattice oxygen mobility during the catalytic redox cycle promotes the interaction between Mo and V, which may result in the formation of definite phases. Indeed, the $Mo_xV_{1-x}O_2$ solid solution was observed by HT-XRD during reduction of calcined MoVP and by LRS (vibrations of Mo–V–O linkages) after catalytic test. It means that the enhancement of catalytic activity and selectivity of MoVP as compared to MoV and Mo catalysts could be due to the formation of mixed (Mo, V) oxides instead of separated V and Mo oxospecies. Mixed oxides like $(Mo,V)_5O_{14}$ or $V_xMo_{1-x}O_{3-0.5x}$ have already been thought responsible of the activity and selectivity to ethene and/or acetic acid [13].

4. Conclusion

Alumina-supported molybdenum catalysts exhibit interesting properties in the oxidative dehydrogenation of ethane to ethene. Both catalytic activity and selectivity to ethene are improved when molybdenum is partially substituted by vanadium, and in the presence of phosphorus the performance increases again. The exact role of P is unknown. However, in its presence, aluminum molybdate crystallises (XRD, LRS), the solid solution $V_xMo_{1-x}O_2$ forms during reduction by hydrogen (HT-XRD), the reducibility is enhanced (TPR, XPS) and more Mo, V, P species are present on the surface (XPS), as compared to the case of Mo and MoV. The greater acidity of Mo (2-propanol decomposition) could be related to more uncovered Al species on surface as compared to MoVP in which most Al is inserted in the bulk as aluminum molybdate. The influence of both vanadium and phosphorus on the properties of molybdenum-based catalyst is plural. Indeed, the vanadium increases the reducibility and the redox (basic) properties of the materials, while the phosphorus could assist the migration of V towards surface. In that way, P would control the reduction of V reduction and probably also would favour the incorporation of some vanadium into molybdenum lattice, as indirectly shown by the formation of $Mo_xV_{1-x}O_2$. Finally, it may also help to ''isolate'' patches of Mo, V oxospecies, the result being a decrease of carbon oxides formation and thus an increase of selectivity to ethene.

Acknowledgements

L. Burylo, M. Frère and L. Gengembre are thanked for performing HT-XRD and XPS experiments.

References

[1] W. Ueda, S.W. Lin, I. Tohmoto, Catal. Lett. 44 (1997) 241.
[2] S. Wang, K. Murata, T. Hayakawa, S. Hamakawa, K. Suzuki, Stud. Surf. Sci. Catal. 130 (2000) 1829.
[3] J.Z. Luo, X.P. Zhou, Z.S. Chao, H.L. Wan, Appl. Catal. A 159 (1997) 9.
[4] Y. Schuurman, V. Ducarme, T. Chen, W. Li, C. Mirodatos, G.A. Martin, Appl. Catal. A 163 (1997) 227.
[5] K. Wada, H. Yamada, Y. Watanabe, T. Mitsudo, J. Chem. Soc., Faraday Trans. 94 (1998) 1771.
[6] F.C. Meunier, A. Yasmeen, J.R.H. Ross, Catal. Today 37 (1997) 33.
[7] P. Ciambelli, P. Galli, L. Lisi, M.A. Massucci, P. Patrono, R. Pirone, G. Ruoppolo, G. Russo, Appl. Catal. A 203 (2000) 133.
[8] E.M. Thorsteinson, T.P. Wilson, F.G. Young, P.H. Kasai, J. Catal. 52 (1978) 116.
[9] M. Merzouki, B. Taouk, L. Tessier, E. Bordes, P. Courtine, in: L. Guczi, et al. (Eds.), New Frontiers in Catalysis, Stud. Surf. Sci. Catal. 75 (1993) 753.
[10] K. Ruth, R. Burch, R. Kieffer, J. Catal. 175 (1998) 27.
[11] D. Linke, D. Wolf, M. Baerns, O. Timpe, R. Schlögl, S. Zeyß, U. Dingerdissen, J. Catal. 205 (2002) 16.
[12] M. Bouchard, M. Roussel, E. Bordes-Richard, K. Karim, S. Al-Sayari, Catal. Today 99 (2005) 77.
[13] M. Roussel, M. Bouchard, K. Karim, S. Al-Sayari, E. Bordes-Richard, Appl. Catal. A: Gen. 308 (2006) 62.
[14] F.G. Young, E.M. Thorsteinson, US Patent No. 4,250,346 (1981).
[15] B. Sulikowski, A. Kubacka, E. Wloch, Z. Schay, V. Cortés Corberan, R.X. Valenzuela, Stud. Surf. Sci. Catal. 130 (2000) 1889.
[16] A.A. Lemonidou, L. Nalbandian, I.A. Vasalos, Catal. Today 61 (2000).
[17] D.I. Enache, E. Bordes-Richard, A. Ensuque, F. Bozon-Verduraz, Appl. Catal. A: Gen. 278 (2004) 103.
[18] L. Tessier, E. Bordes, M. Gubelmann-Bonneau, Catal. Today 24 (1995) 335.
[19] M. Merzouki, E. Bordes, B. Taouk, L. Monceaux, P. Courtine, Stud. Surf. Sci. Catal. 72 (1992) 81.
[20] J.M. Lopez Nieto, V.A. Zazhigalov, B. Solsona, I.V. Bacherikova, Stud. Surf. Sci. Catal. 130 (2000) 1853.
[21] T. Katou, D. Vitry, W. Ueda, Catal. Today 91–92 (2004) 237.
[22] J.M. López-Nieto, P. Botella, P. Concepció, A. Dejoz, M.I. Vásquez, J. Catal. 209 (2002) 445.
[23] C. Stinner, R. Prins, Th. Weber, J. Catal. 191 (2000) 438.
[24] E. Payen, R. Hubaut, R. Kaztelan, S. Poulet, J. Catal. 147 (1994) 123.
[25] M.A. Bañares, S.J. Khatib, Catal. Today 96 (2004) 251.
[26] D.A. Morris, C. Kaidong, A.T. Bell, E. Iglesia, J. Catal. 208 (2002) 139.
[27] G. Mestl, J. Raman Spectrosc. 33 (2002) 333.
[28] G. Mestl, T.K.K. Srinivasen, Catal. Rev.-Sci. Eng. 40 (1998) 451.
[29] A. Neiman, S. Barsanov, J. Solid State Electrochem. 5 (2001) 382.

[30] B. Reddy, B. Chowdhury, E. Reddy, A. Fernandez, Appl. Catal. A: Gen. 213 (2001) 279–288.
[31] N.K. Nag, J. Phys. Chem. 91 (1987) 2324.
[32] N.K. Nag, E.E. Massoth, J. Catal. 124 (1990) 127.
[33] J. Haber, A. Kozlowska, R. Kozlowski, J. Catal. 102 (1986) 52.
[34] P. Atanasova, J. Uchytil, M. Kraus, T. Halachev, Appl. Catal. 65 (1990) 53.
[35] J.A.R. VanVeen, P.A.J.M. hendriks, R.R. Romers, E.J.G.M. Romers, A.E. Wilson, J. Phys. Chem. 94 (1990) 5282.
[36] E.C. DeCanio, J.C. Edward, T.R. Scalzo, D.A. Storm, J.W. Bruno, J. Catal. 132 (1991) 498.
[37] D. Chadwich, D.W. Aitchison, R. Badilla-Ohlbaum, L. Josefsson, Stud. Surf. Sci. Catal. 16 (1983) 323.
[38] D.J. Sajkowski, J.T. Miller, G.W. Zajag, Appl. Catal. 62 (1990) 205.
[39] A. Lopez-Cordero, N. Esquivel, J. Lazaro, J.L.G. Fierro, A. Lopez Agudo, Appl. Catal. 48 (1989) 341.
[40] R. Lopez Cordero, F.J. Gil Liambias, A. Lopez Agudo, Appl. Catal. 74 (1991) 125–136.
[41] M.R. Smith, L. Zhang, S.A. Driscoll, U.S. Ozkan, Catal. Lett. 19 (1993) 1.
[42] A. Erdohelyi, F. Solymosi, J. Catal. 123 (1990) 31.
[43] M.C. Abello, M.F. Gomez, O. Ferretti, Appl. Catal. A: Gen. 207 (2001) 421.
[44] G. Busca, E. Finocchio, G. Ramis, G. Ricchiardi, Catal. Today 32 (1996) 133.
[45] J.C. Védrine, J.M.M. Millet, J.C. Volta, Catal. Today 2 (1996) 115.